

Article

Improved Isothermal Relaxation Current Measurement Based on Isolated Circuit for Nondestructive Evaluation of High-Voltage Cable Insulation

Huangjing Gu ¹, Yongkang Zhang ¹, Bin Shen ¹, Ziqi Liu ¹, Yunjie Zhou ¹, Xiaodi Wang ¹, Xinyang Zhu ² and Yalin Wang ^{2,*} 

¹ State Grid Shanghai Cable Company, Shanghai 200122, China

² Department of Electrical Engineering, School of Electronic Information and Electrical Engineering, Shanghai Jiao Tong University, Shanghai 200240, China

* Correspondence: wangyalin2014@sjtu.edu.cn

Abstract: The Isothermal Relaxation Current (IRC) method, as a non-destructive condition evaluation method based on insulation dielectric response, has been applied in the maintenance of power cables. However, the relaxation current is usually conducted through the outer shield of the high-voltage wire, which will introduce the extra depolarization current into the test circuit, affecting the accuracy of the test results. Furthermore, most IRC cable measurements are single-phase, which means depolarization currents are measured for each cable separately. In order to improve the measurement accuracy and efficiency of the IRC test, this paper proposes an improved IRC measurement method based on an isolated circuit, which discharges the interference current from the high-voltage insulated wire back to the earth and reduces the measurement error of depolarization current. At the same time, a three-phase IRC simultaneous test system is designed, and the control software is developed. Furthermore, by verifying the accuracy of the test system, the independence of the single-phase circuit and the consistency of the three-phase circuit is achieved. The effect of depolarization time and temperature on the relaxation current is then explored to determine the suitable parameter of the IRC test. Finally, the IRC system is used to evaluate the aging state of 10 kV cables with various aging conditions in the air and water for the longest 12 months. Critical parameters such as aging factor and time constants are compared to investigate the aging characteristics of tested cables with various aging conditions in the air and water. The proposed method and research conclusions can provide helpful references for the non-destructive condition evaluation for high-voltage cable insulation.

Keywords: high-voltage cable insulation; condition evaluation; non-destructive measurement; isothermal relaxation current; isolated circuit



Citation: Gu, H.; Zhang, Y.; Shen, B.; Liu, Z.; Zhou, Y.; Wang, X.; Zhu, X.; Wang, Y. Improved Isothermal Relaxation Current Measurement Based on Isolated Circuit for Nondestructive Evaluation of High-Voltage Cable Insulation. *Energies* **2023**, *16*, 7892. <https://doi.org/10.3390/en16237892>

Academic Editor: Javier Contreras

Received: 29 October 2023

Revised: 18 November 2023

Accepted: 25 November 2023

Published: 3 December 2023



Copyright: © 2023 by the authors. Licensee MDPI, Basel, Switzerland. This article is an open access article distributed under the terms and conditions of the Creative Commons Attribution (CC BY) license (<https://creativecommons.org/licenses/by/4.0/>).

1. Introduction

1.1. Condition Evaluation of Cable Insulation

Polymer-insulated cables have gradually become an important part and key equipment for power transmission in power systems due to their excellent electrical insulation properties and light weight [1–4]. However, insulation aging and degradation of cables will inevitably occur during long-term service, affected by electrical, thermal, mechanical, and other environmental factors, which increases the probability of cable failure and affects the safe operation of the power grid. Therefore, it is of great significance to detect and evaluate the insulation status of power cables.

Cable insulation evaluation aims to evaluate cable insulation performance by analyzing cable characteristics. Therefore, the selected characteristic features should be related to the cable insulation performance. Characteristic features can be divided into direct characteristic features and indirect characteristic features. Direct characteristic features

include mechanical strength, breakdown field strength, etc. These characteristics are relevant parameters that can directly reflect the cable insulation performance; for indirect characteristic features, the features and the connection between features and performance often need to be determined first. There are many technical methods for cable insulation testing, which can be classified differently according to different standards. Detection technology includes offline detection and online detection, which are classified according to the method of application. Detection technology can also be divided into destructive testing and non-destructive testing, classified according to whether the test causes the sample to be damaged.

Destructive testing methods can cause damage to the insulation, shorten the life of the cable, or even cause direct failure. Therefore, it is crucial to study non-destructive testing methods for cable insulation condition detection. Non-destructive testing methods mainly include partial charge test, dielectric response test, insulation resistance, or leakage current test. At present, it is generally believed that there is a close relationship between the aging of cable insulation and cable partial discharge [5–7]. However, during actual operation, affected by factors such as transmission distance, the intensity of the PD signal may be very weak. At the same time, the PD sensor is easily affected by interference from other signals in the environment, making the detected signals more complex and making analysis more difficult. The reliability of partial discharge signals is questionable. As for the dielectric response test, the dielectric loss $\tan\delta$ is generally used to characterize the energy loss of the material during the polarization process [8–10]. A large number of studies have shown that $\tan\delta$ can effectively reflect the state of the cable during operation, such as the water absorption status, cavities, etc. In addition, the insulation resistance of the insulation material can effectively reflect the insulation characteristics of the material. In the case of DC, the insulation resistance of the cable can be calculated using the conduction current of the cable [11,12], and the type of cable defects can be determined by the cable insulation resistance value. However, some small defects have little effect on insulation resistance, and insulation resistance cannot effectively distinguish these small defects.

1.2. Isothermal Relaxation Current Method for Nondestructive Evaluation

The isothermal relaxation current method is a relatively new method for evaluating the condition of insulation materials. Without causing damage to the medium, it can measure the depolarization current of the cable, which can effectively evaluate the aging condition of the insulation and has high repeatability [13]. This method uses the relaxation and depolarization phenomena of the insulation material during the depolarization process [14] to evaluate the aging degree and internal defects of the cable.

Researchers proposed the theory of trap energy levels and isothermal relaxation currents as early as the last century and explored the relationship between trap energy level distribution and depolarization current in insulating media [15]. Furthermore, based on the IRC theory, scholars analyzed the different physical processes that constitute dielectric insulation polarization, and for the first time gave the calculation method and analytical formula of the aging factor A. They also verified the IRC test and the relationship between the aging factor A and the cable aging degree through experiments. In addition, some researchers used a third-order exponential model to fit the IRC curve through experiments on a large number of cables in operation, gave the specific steps and methods of IRC analysis, and verified the effectiveness of the method, with an error rate lower than 0.5% [16].

Compared with traditional cable insulation evaluation, as shown in Table 1, the isothermal relaxation current method has great advantages in terms of anti-interference, test voltage, detection range, detection time, and destructiveness.

At present, most IRC cable measurements are single-phase, and this method requires depolarization current measurement for each cable separately. In field testing, if each phase cable is still measured in sequence, the power outage will be too long, which will affect the reliability of the power supply. At the same time, uncontrollable factors such as temperature and humidity on site may change at any time. External factors vary during

measurement, which will largely affect the accurate determination of the cable insulation status. Furthermore, the depolarization current is usually conducted through the outer shield of the high-voltage line, which will introduce the depolarization current of the high-voltage line insulation into the test circuit, affecting the accuracy of the test results. Therefore, it is necessary to solve the problem above and improve the IRC measurement.

Table 1. Comparison of different cable evaluation methods.

Method	Anti-Interference	Applied Voltage	Test Range	Test Time	Destructive
Infrared spectrum	High	No	Local	Long	Yes
Differential Scanning Calorimetry	High	No	Local	Long	Yes
Thermogravimetric analysis	High	No	Local	Long	Yes
Hardness	High	No	Local	Long	Yes
Elongation at break	High	No	Local	Long	Yes
Insulation resistance method	Low	High	Overall	Short	No
partial discharge method	Low	High	Overall	Short	No
dielectric loss tangent	Low	Low	Overall	Short	No
Voltage endurance test	Low	High	Overall	Long	Yes
DC leakage current method	Low	High	Overall	Short	Yes
Dielectric spectroscopy	Low	Low	Overall	Long	No
0.1 Hz voltage endurance test	Low	High	Overall	Long	Yes
Isothermal relaxation current	High	Low	Overall	Short	No

1.3. Contribution of This Paper

This paper proposes an improved IRC measurement method based on an isolated circuit and simultaneously measures the IRC of three-phase high-voltage cables. In view of the existing technical problems, the three-phase synchronous IRC test system was improved by separating the polarization loop and depolarization test loop to eliminate the interference of the transmission line. Then the consistency of test results between the single-phase loop and the three-phase test was verified. The influence of depolarization time and test temperature on the isothermal relaxation current test is further explored to determine the suitable parameter of the IRC test. Finally, a three-phase synchronous IRC test was carried out to evaluate the aging status of the cable in water and air.

2. Basic Method of IRC

2.1. Basic Principles of Dielectric Polarization and Depolarization

Under the application of an external electric field, the dielectric material will be polarized. When the dielectric material is in a uniform electric field $E(t)$, the current density inside it is [17]

$$H(t) = \sigma E(t) + \frac{dD(t)}{dt} \quad (1)$$

where σ is conductivity, and $D(t)$ is electrical displacement.

$$D(t) = \epsilon E(t) + P \quad (2)$$

where ϵ is the dielectric constant and P is the polarization intensity:

$$P = \epsilon_0(\epsilon_\infty)E(t) + \epsilon_0 \int_0^t f(t)E(t - \tau)d\tau \quad (3)$$

where ε_∞ is the high-frequency component of the dielectric constant. Substituting Equations (1) and (2) into Equation (3), we obtain:

$$H(t) = \sigma E(t) + \varepsilon_0 \varepsilon_\infty \frac{dE(t)}{dt} + \varepsilon_0 \frac{d}{dt} \int_0^t f(t-\tau) E(t-\tau) d\tau \quad (4)$$

When the applied voltage is $U(t)$, the expression of $i(t)$ is:

$$i(t) = H(t) \times s = C_0 \left[\frac{\sigma}{\varepsilon_0} U(t) + \varepsilon_\infty \frac{dU(t)}{dt} + \frac{d}{dt} \int_0^t f(t-\tau) U(t-\tau) d\tau \right] \quad (5)$$

where $C_0 = \varepsilon_0 s / d$, $U(t) = E(t) \cdot d$, s is the area of the test sample, and d is the thickness of the test sample.

When voltage U_0 is applied at time 0, the current in the sample is:

$$i_{pol} = C_0 U_0 \left[\frac{\sigma}{\varepsilon} + f(t) \right] \quad (6)$$

After a period of polarization t_p , U_0 is removed and the sample is short-circuited. The depolarization current can be obtained as:

$$i_{depol} = C_0 U_0 [f(t) - f(t + t_p)] \quad (7)$$

The measurement loop and the corresponding typical relaxation curve are shown in Figure 1. To ensure that there is no charge remaining in the sample, a step voltage signal with an amplitude U_p is applied to the sample to generate the polarization current i_p , where i_p consists of the DC conductivity current and the sample polarization current. After the polarization process is completed, the sample voltage is reduced to zero and short-circuited. The internal charges escape from the traps and become free charges, thereby generating a depolarization current i_d .

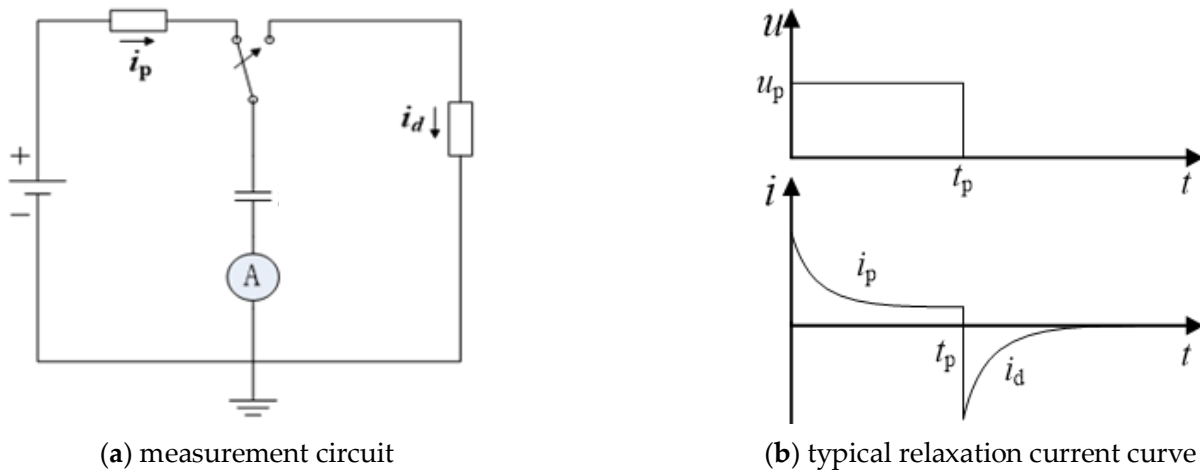


Figure 1. Measurement circuit of relaxation current and typical curve.

2.2. Theory of Isothermal Relaxation Current

The dielectric will respond to a weak current under the polarization of a DC electric field. Relaxation currents are formed under polarization or depolarization. J.G. Simmonds et al. proposed the isothermal relaxation current theory. In polymers, the trap distribution exhibits discontinuous characteristics and is discretely distributed throughout the energy band range [15]. Due to this distribution characteristic, electrons occupy traps above the Fermi level, while a large number of holes occupy traps below the Fermi level. Therefore,

only the trap region above the Fermi level needs to be involved in practical research. The function $G_N(W,t)$ shows the relationship between trap energy levels and current:

$$G_N(W,t) = e_N(W,t) \cdot e^{-e_N(W,t) \cdot t} \tag{8}$$

$$e_N = v \cdot e^{\frac{W_H - W_C}{k \cdot T}} \tag{9}$$

where e_N is the probability of emitting electrons from the trap energy level to the conduction band, W_C is the conduction band energy, v is the escape frequency, W_H is the trap energy, K is the Boltzmann constant, and T is the temperature. A “bell”-shaped distribution curve can be obtained from the functional expression $G_N(W,t)$, and $G_N(W,t)$ reaches the maximum value at W_H , as shown in Figure 2.

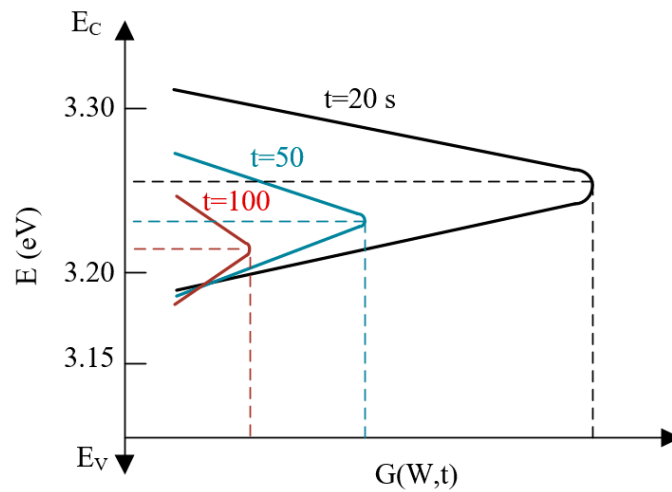


Figure 2. $G_N(W,t)$ as a function of energy at various times.

The energy of the detrapped electron is approximately W_H , and the trap energy level gradually transits from the conduction band to the Fermi level as time increases. When the trap energy is higher than W_H , the electrons will escape and become free electrons. For traps with energy lower than W_H , the trapped electrons will not escape and remain bound in the trap. The expression of trap depth $W_T(t)$ is shown in Equation (10), where $W_T(t)$ and $I_n(t)$ have an approximately linear relationship.

$$W_T(t) = W_C - W_H = k \cdot T \cdot \ln(v \cdot t) \tag{10}$$

Under constant temperature conditions, the expression of depolarization current in the dielectric is:

$$I(t) = \frac{qLkT}{2t} f_0(E) \cdot N(W_H) \tag{11}$$

where L is the thickness of the tested sample, q is the charge quantity, $f_0(E)$ is the initial occupancy probability of the trap, $N(W_H)$ is the trap density, and the expression of $f_0(E)$ is as follows:

$$f_0(E) = \frac{v\sigma_n n_s}{v\sigma_n n_s + v\sigma_p p_s} \tag{12}$$

where σ_n and σ_p are the capture cross-sections, and n_s and p_s are the positive and negative charge densities. Therefore, the parameter $f_0(E)$ is only statistical information and irrelevant to the energy distribution of the trap. Furthermore, it is assumed that the distribution of electron traps is the same as that of hole traps, that is, the initial occupancy probability $f_0(E)$ is equal to 0.5. Therefore, the electron current is equal to the hole current. Combining Equations (10) and (11), it can be seen that the trap density has a positive correlation with $I \cdot t$, and the trap depth and $I_n(t)$ also conform to this positive relationship. Therefore, the

use of isothermal relaxation current curves can effectively evaluate the trap distribution in cable insulation.

2.3. Aging Model of Cable Insulation

The physical processes such as dielectric response are parameterized, and the equivalent circuit of cable insulation is given, as shown in Figure 3. Among them, the three forms of cable polarization are shown in the dotted box. R_s is the cable shield resistance, R_i and C_i are the resistance and capacitance of the cable insulation, respectively, R_p is the protection resistance, R_c is the discharge resistance, and R_m is the measurement resistance.

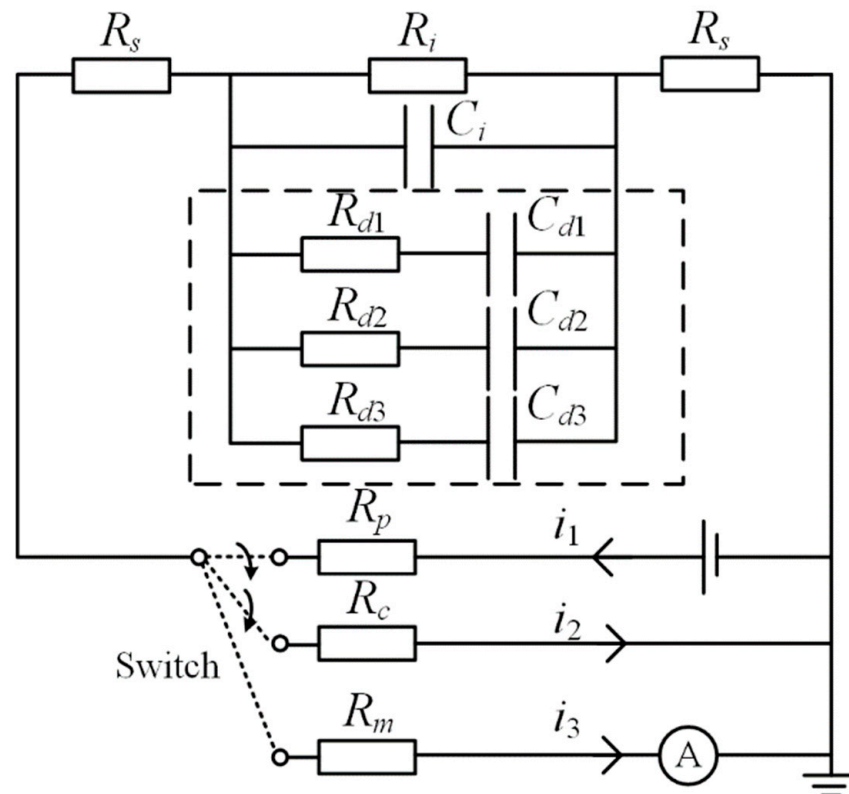


Figure 3. Equivalent circuit of the dielectric response of the cable.

The impact of insulation aging on dielectric depolarization current can be obtained by building a dipole circuit simulation. Therefore, classified resistance–capacitance–equivalent circuits can be used to characterize different polarization processes of cable insulation. Among them, the three RC branches represent dielectric body polarization, interface polarization, and polarization determined by insulation aging. Fit the current $I(t)$ [4,18]:

$$I(t) = I_0 + \sum_{i=1}^3 a_i \cdot e^{-\frac{t}{\tau_i}} \quad (13)$$

where t is time, I_0 is the current value when the current reaches a steady state, and a_i and τ_i are parameters related to the insulation state, reflecting the trap density and trap depth, respectively. The third-order index corresponds to three polarization processes.

The aging factor A is generally used to evaluate the aging state of insulation. The calculation method is as follows [19]:

$$A = \frac{Q(\tau_3)}{Q(\tau_2)} \quad (14)$$

where $Q(t)$ is the integral of $I(t)$ with respect to time:

$$Q(t) = \int_0^t I(t)dt \quad (15)$$

Substituting Equation (13) into Equation (15), we obtain:

$$Q(t) = I_0 \cdot t - \sum_{i=1}^3 a_i \tau_i e^{-\frac{t}{\tau_i}} + \sum_{i=1}^3 a_i \tau_i \quad (16)$$

In the depolarization current results, each current component generally exhibits the following characteristics:

$$I_0 \cdot t \approx 0 \quad (17)$$

$$\tau_2 > 3\tau_1, \tau_3 > 3\tau_2 \quad (18)$$

Substituting $t = \tau_2$ and $t = \tau_3$ into Equation (16), we obtain:

$$Q(\tau_2) \approx a_1 \tau_1 + a_2 \tau_2 \left(1 - \frac{1}{e}\right) + a_3 \tau_3 \left(1 - e^{-\frac{\tau_2}{\tau_3}}\right) \quad (19)$$

$$Q(\tau_3) \approx a_1 \tau_1 + a_2 \tau_2 \left(1 - e^{-\frac{\tau_3}{\tau_2}}\right) + a_3 \tau_3 \left(1 - \frac{1}{e}\right) \quad (20)$$

In the aging criteria given by German scholars, when the aging factor $A < 1.75$, the insulation condition of the cable is good. When $1.75 < A < 1.90$, the insulation aging is not obvious. When $1.90 < A < 2.10$, the insulation aging phenomenon is obvious. When $A > 2.10$, the insulation deteriorates badly [16].

However, relevant research shows that the aging factors of Chinese-made cables are generally larger than the reference values given from other countries. Therefore, the reference values obtained by our group after a large number of tests are given here. When the cable has not yet aged and maintains good insulation performance, $A < 2.0$. When the insulation is initially aged, $2.0 < A < 2.4$. When the insulation is obviously aged, $2.4 < A < 2.8$, and when the cable insulation deteriorates badly, the cable needs to be replaced in time, $A > 2.8$.

3. Improved IRC Measurement System

3.1. Modified IRC Method Based on Isolated Circuit

The test site will interfere with the IRC measurement of cable insulation, which will not only cause current measurement errors, but also affect the operation of the measurement system. Generally speaking, interference sources are mainly divided into three categories: electromagnetic interference, power supply interference, and test system interference.

Electromagnetic interference mainly comes from large electrical equipment on site, such as high-voltage wires, relays, etc. To suppress such interference, the modules of the IRC test system are integrated into reliably grounded metal boxes. At the same time, the current transmission line uses a coaxial cable with a shielded net. In order to eliminate the influence of power frequency voltage fluctuations, an isolation transformer is installed to isolate the power supply side of the system from the grid side. Both types of interference are random interference and can occur at any stage of the IRC test, but the duration of the interference is relatively short.

During IRC testing, some components of the test system may induce a depolarization current, which flows into the measurement circuit and affects the measurement results. This kind of interference belongs to system interference. The test system interference is mainly generated from the high-voltage lines with silicone rubber insulation. In addition, the equivalent circuit, including the high-voltage wire, is shown in Figure 4. The high-voltage wire is modeled as a parallel structure of R_l and C_l and is grounded through air, and its parameters are simplified to C_{air} . In Figure 4, not only is the tested cable insulation layer

polarized, but the high-voltage insulated wire is also polarized during the polarization process. Therefore, the polarization current can be expressed as $i_1 + i_{pline}$. During the depolarization process, the depolarization current released by the high-voltage insulated wire enters the measurement circuit in series, and the depolarization current measured is $i_3 + i_{dline}$. Therefore, the depolarization current of high-voltage insulated wires probably affects the IRC measurement results.

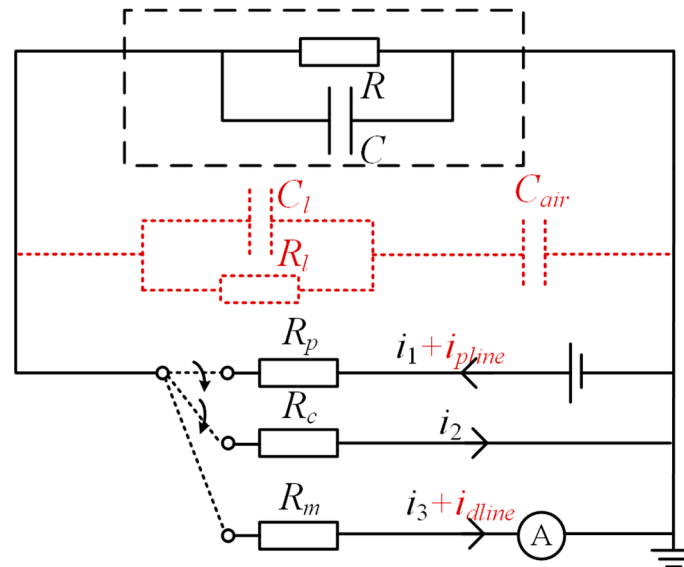


Figure 4. Equivalent circuit of IRC measurement considering system interference.

This paper proposes an improved IRC method based on an isolated circuit. The equivalent circuit is shown in Figure 5. The high-voltage wire is a shielded coaxial cable, the core conducts high voltage, and the outer shield is grounded. Additionally, the copper shield of the cable is connected to the ground via a current-measuring instrument. During the polarization process, the high-voltage wire and the tested cable are polarized at the same time. During the depolarization process, the depolarization current released by the cable insulation will be collected by the current-measuring instrument through loop 1, while the depolarization current of the high-voltage wire is released from loop 2 and will not be captured by the instrument. Therefore, based on this method, the depolarization current generated by high-voltage wires is excluded, and the depolarization current signal of the tested cable is obtained through the current measuring instrument.

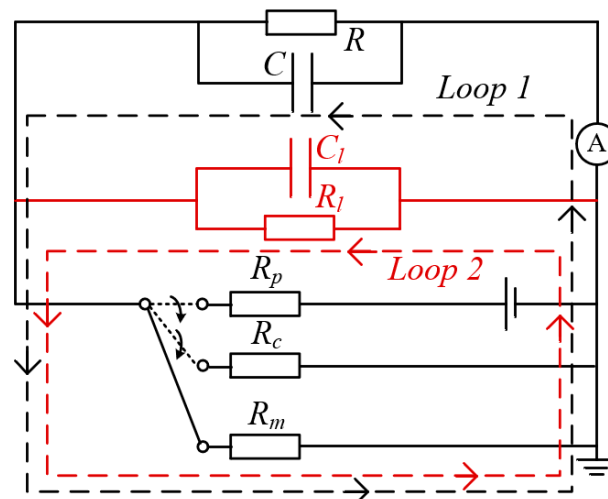


Figure 5. Equivalent circuit of the modified IRC method based on isolated circuit.

3.2. Three-Phase Simultaneous Measurement System

Based on the isolated circuit method, a three-phase IRC simultaneous measurement system is established, as shown in Figure 6. The functions that this test system can implement include the controllable output of polarization voltage, automatic switching of measurement loops, and pico-current signal amplification and storage. Each module is packaged in a metal shielding box to facilitate integrated control and is equipped with status indicators to display the test status.

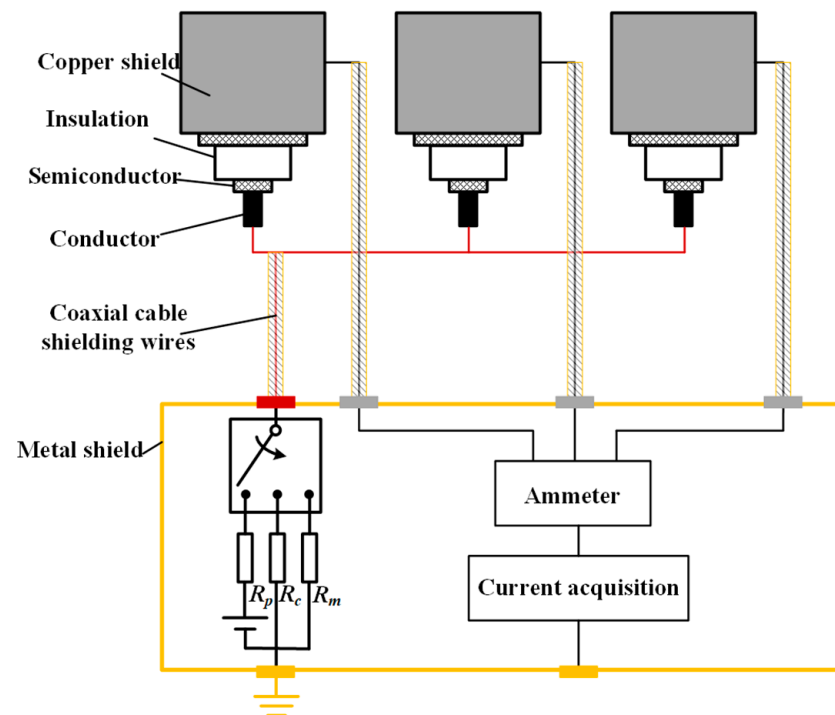


Figure 6. Three-phase IRC simultaneous measurement system.

3.3. Verification of the Measurement System

This test system can achieve a synchronized collection of depolarization currents, but it must ensure that the three-phase currents do not affect each other during the measurement process so that the measurement results can reflect the actual insulation conditions of each phase cable. Therefore, the current measurement circuits of this system should not cross each other, that is, it must be ensured that the current measurements of each phase do not interfere with each other.

A 10 kV cable with cross-linked polyethylene (XLPE) insulation was used to verify the performance of the test system. The outer shielding layer was peeled off for 20 cm at both ends of the cable. The dirt on the insulation surface was removed and grounding protection rings were applied at both ends of the cable to reduce the impact of the leakage current. A DC high voltage is applied to the tested cable. One phase of the measurement circuit is connected to the cable copper tape. The input terminals of the remaining two phases are left floating. The polarization voltage is set to 1000 V. The polarization and depolarization times are both 300 s. The three-phase cables were short-circuited for at least 12 h before testing.

The depolarization current measurement results of each phase are shown in Figure 7. It can be seen that the three-phase measurement results are independent of each other. When a certain phase current circuit is connected to the cable load, the phase will be measured with depolarization current, while the other two phases without load will not generate a depolarization current signal, and the current is basically maintained at 0 pA. If phase A is connected to the cable, the current in phase A will attenuate significantly within the first 50 s of depolarization, and within the next 250 s, the current value will be stable, with its

value fluctuating around 0 pA, while the measurement results of the two phases B and C do not contain depolarization current, and the current remains at about 0 pA. In addition, it can be seen from the comparison of depolarization currents of each phase in Figure 7d that the depolarization currents of different phases obtained in different test circuits are basically the same, and the steady-state current is basically 0 pA, which meets the requirements of the test system. The above results show that the three-phase current measurements of the test system are independent of each other and verify the consistency between each phase.

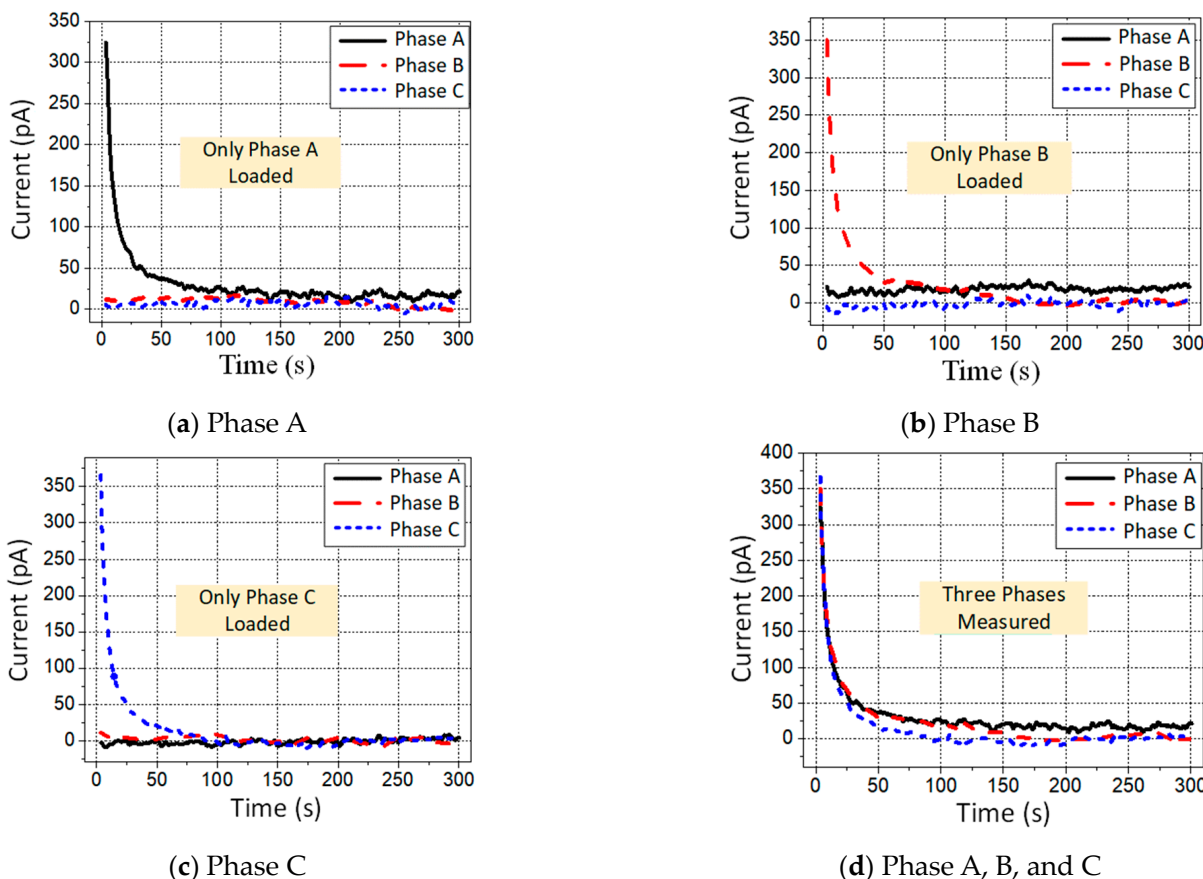


Figure 7. Verification of the three-phase measurement system.

4. Experiment Results

4.1. Influence Factor of IRC Experiment

In IRC measurement, there is no clear reference standard for the selection of test parameters, such as polarization time t_p . It is generally believed that the longer the test, the more accurate the results. Since the IRC test is an off-line detection technology for cable outages, long-term outages will affect the power supply reliability of the power grid, and can hardly meet the needs of field cable testing. Therefore, reasonable parameters of depolarization time and other parameters in the process of cable IRC measurement are of great significance to realize the field application of the IRC method and improve the test efficiency. In addition, the detection of three-phase cables is usually carried out one by one, so it takes a long time to complete the measurement of three cables, during which the ambient temperature may change greatly. Temperature will be another key factor affecting the cable IRC measurement. So it is necessary to discuss the influence of depolarization time and temperature on IRC measurement to provide a basis for the selection of IRC experiment parameters.

4.2. A. Depolarization Time

In order to explore the effect of depolarization time t_d on IRC tests, the value range of depolarization time is 300~3000 s, specifically 300, 600, 900, 1200, 1500, 2000, 2500, and 3000 s. The polarization time is 1500 s. The measured depolarization current was fitted by Equation (13). The results are shown in Figure 8. It illustrates that peak 3 tends to move to the right as the depolarization time increases. When the depolarization time is 300 s, the time of peak 3 is less than 100 s, while the time of peak 3 is close to 1000 s when the depolarization time reaches 3000 s. On the whole, when the depolarization time is less than 900 s, peak 3 will shift to the right with the increase in the depolarization time. However, when the depolarization time is greater than 1200 s, the partial peak curve of the relaxation current is mainly distributed on the larger time axis, and the distribution is relatively stable.

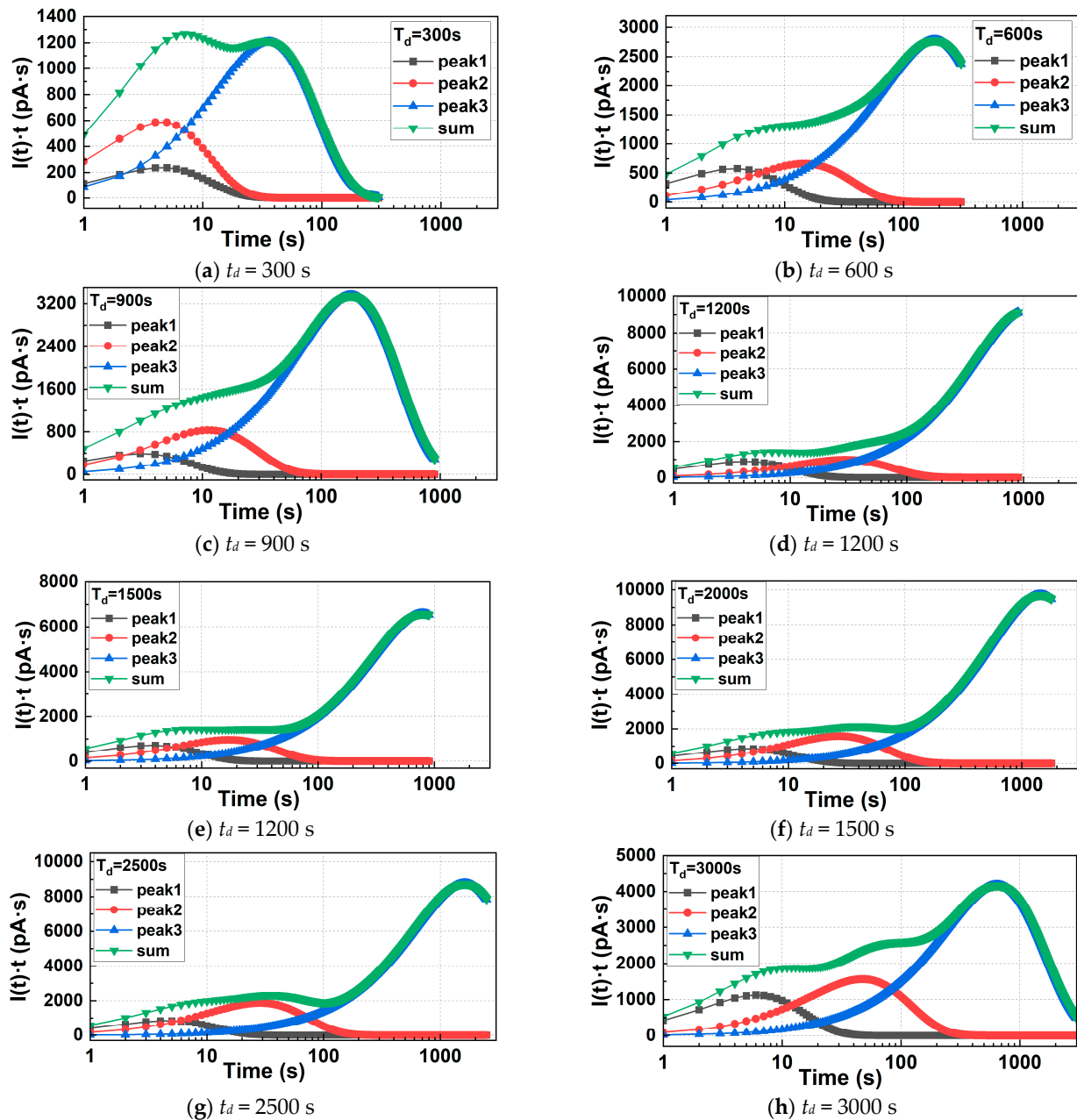


Figure 8. Effect of depolarization time on depolarization current.

Therefore, when the depolarization time is short, the fitting peak results are concentrated in the smaller interval in time. With the increase in depolarization time, the distribution interval of the sub-peak curve increases, and when the depolarization time exceeds 1200 s, the distribution of the fitted wind is basically stable.

The length of depolarization time does not influence the dielectric response of the insulation during the short circuit. It determines the amount of IRC data, which will greatly affect the fitting results. According to IRC theory, the measurable trap density is related to the depolarization time. So the depolarization time needs to be extended to further characterize the trap with greater depth. According to Figure 8, the variation curve of the time constant $\tau_1 \sim \tau_3$ with the depolarization time is given, as shown in Figure 9. The fitted time constant increases with the growth of depolarization time, and the time constant τ_3 shows the most obvious increase. The extension of depolarization time will improve the fitting accuracy, but more test data are also accompanied by more complex interference, such as ground potential fluctuations resulting in data offset. These random interferences during the long testing process affect the accuracy of the fitting results.

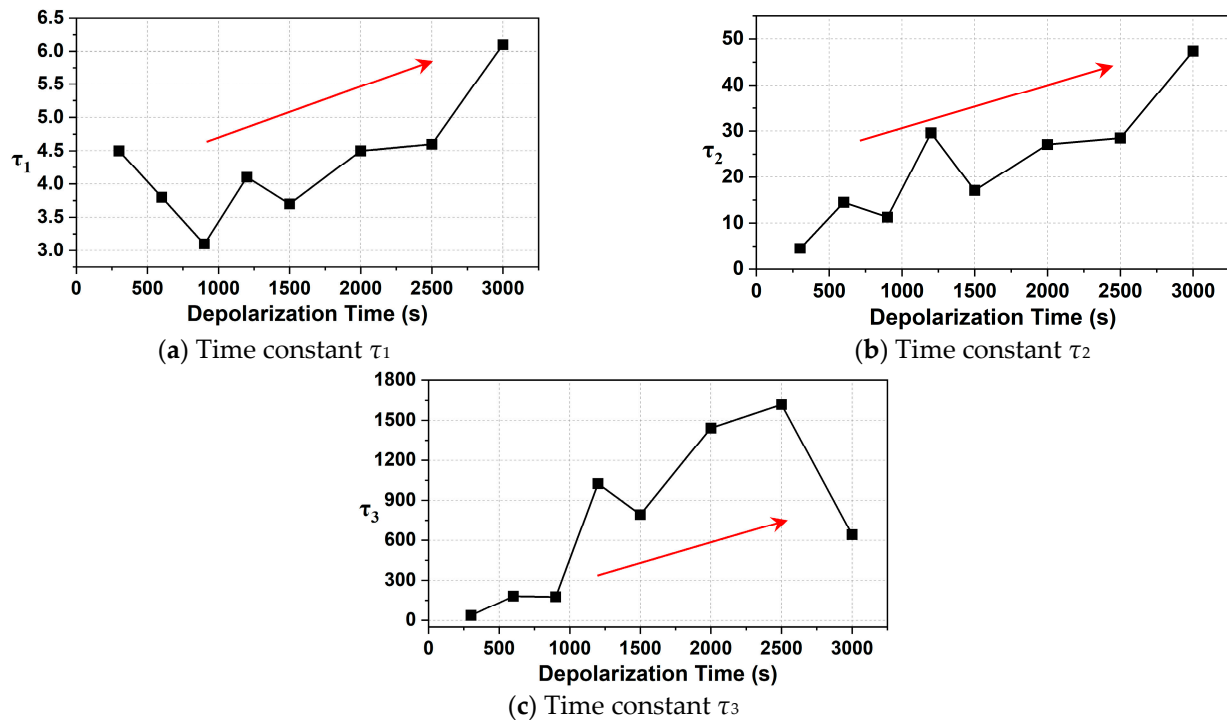


Figure 9. Effect of depolarization time on time constant.

Furthermore, the aging factor A calculated from the IRC measurement is the most intuitive parameter to judge the insulation status. Aging factor A of different depolarization times was obtained according to Equation (14), as shown in Figure 10.

It can be seen from Figure 10 that aging factor A first increases and then decreases with the increase in depolarization time. In the range of 1200–2500 s, the value of A fluctuates slightly, with an average value of about 4.2. Theoretically, accurate results can be obtained when the depolarization time is set within this range. In the actual field test, long-time depolarization is easily affected by the environment, and the cable outage time is too long to meet the requirements of power supply reliability. Therefore, considering the accuracy of test results and test efficiency, the more suitable depolarization time t_d is in the range of 1200–1800 s.

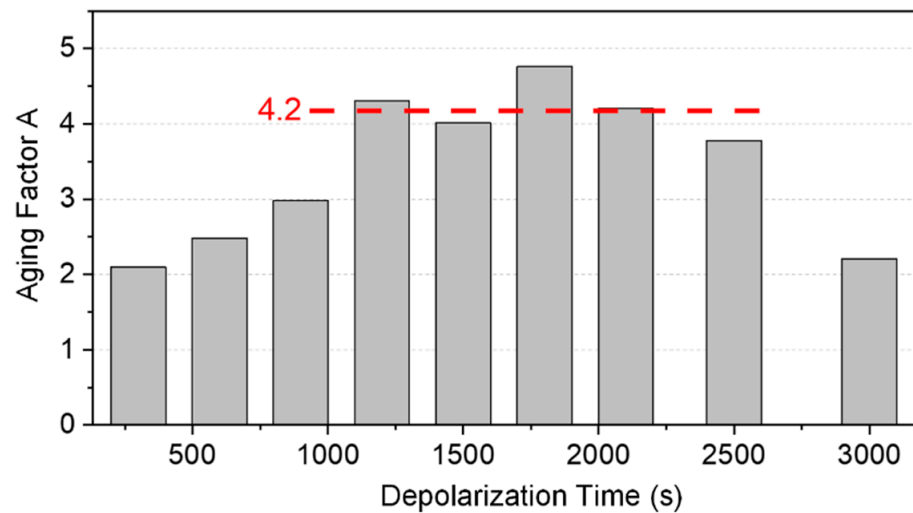


Figure 10. Diagram of the change in aging factor A with depolarization time t_d .

4.3. B. Temperature

To investigate the influence of temperature on the IRC test, the temperature control of cable insulation is realized by a silicone rubber-insulated flexible heating belt combined with a thermocouple and temperature controller. The polarization voltage is 1 kV, and the polarization and depolarization time are 1800 s, respectively. The measured temperature is 30, 50, 70, and 90 °C. Before the test, the cable was preheated for 5 min to ensure that the temperature distribution inside the cable insulation was uniform.

The depolarization current curve at different temperatures is shown in Figure 11. When the temperature rises, the current has a tendency to decrease first and then increase. The maximum current at 50 °C is less than that at 30 °C. When the temperature is higher than 50 °C, the maximum value of the depolarization current rises with the increase in temperature. It indicates that the effect of temperature on depolarization current is prominent, and the mechanism of current at various temperatures is complicated. When the temperature is low, the depolarization current decreases with the increase in temperature, while in the higher temperature range, the depolarization current has a positive temperature characteristic.

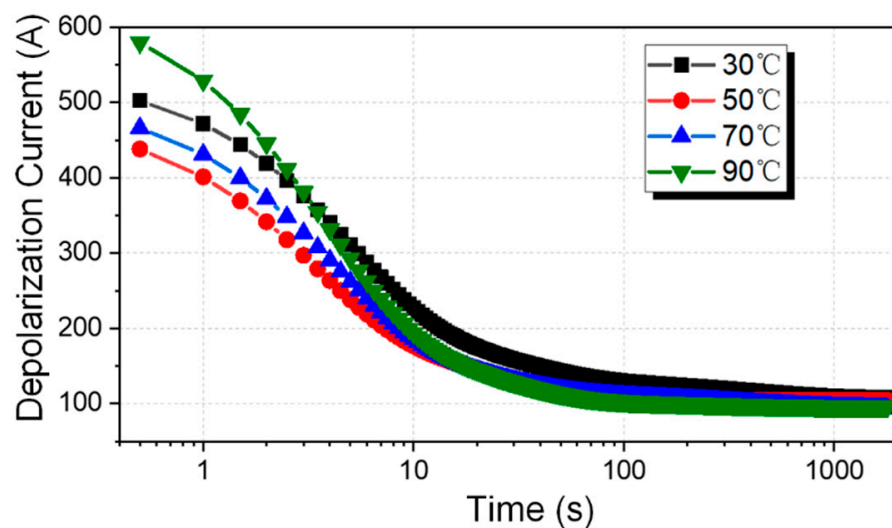


Figure 11. Effect of temperature on relaxation current.

The effect of temperature on depolarization current is essentially the effect on the migration and detrapping process of charge. At lower temperatures, the trapped charge is released during depolarization, resulting in a relaxation current. As the temperature increases, the detrapping coefficient of charge increases, and a large number of charges in shallow traps escape, so the trapped charge decreases. In the lower temperature range, the increase in temperature leads to a decrease in the amount of trapped charge, resulting in a decrease in the depolarization current.

At a higher temperature range (50~90 °C), the depolarization current increases significantly. The material conductivity increases and the deep trap charge is prone to depolarization when the temperature is higher. On the one hand, with the increase in temperature, the conductivity of XLPE material increases, and the resistance of the insulating medium decreases, so that the depolarization current increases. On the other hand, at higher temperatures, the temperature will further affect the detrapping behavior of the deep trap charge, so the temperature increase will accelerate the detrapping of the charge in the deep trap. According to the thermal stimulation current theory, the available trap depth ΔE by experiment will increase with the rise in the test temperature. The trap depth ΔE is:

$$\Delta E = \frac{2.47T^2k}{w} \quad (21)$$

where T is the temperature when the thermal stimulation current reaches its peak, and w represents half the peak current width. It can be seen that high temperature makes charges in deep traps more likely to detrapping in the depolarization process, increasing the depolarization current.

4.4. IRC Measurement Results of Aging Conditions

The operating environments of cables are complicated, which directly affects the lifetime of cables. The improved test system was used for the isothermal relaxation current test to explore the aging assessment of cables in various laying environments. Before the test, the 10 kV power cables were electrothermally aged in air and water to represent the cables used in different laying environments. Aging times are 6 months and 12 months, respectively. Continuous current is applied to the cable laid in the air to heat the cable to 90 °C during the aging process. At the same time, the same current was applied to the cable in the water for comparison. Five conditions of cables are taken for investigation: unaged cables, cables aged for 6 months and 12 months in air, and cables aged for 6 months and 12 months in water.

The applied polarization voltage was 1 kV. According to Section 4.1, the polarization and depolarization times were both 1800 s, and the temperature was set to 30 °C. Before IRC testing, the samples were short-circuited for 24 h to reduce the effects of residual charges in the insulation during the aging and treatment process.

The measured depolarization current is shown in Figure 12. It can be seen that the initial current increases after the cable is aged in the air for a long time. The IRC curve of water aging samples appears to be more complicated. With aging in water, the initial IRC value first increases and then decreases significantly. Regardless of the aging environment, aging will effectively slow down the decline of the depolarization current, thereby increasing the time required for the IRC to reach equilibrium.

Furthermore, in order to explore the characteristics of the depolarization current, the IRC curve was fitted according to Equation (13), and the fitting results are shown in Figure 13. The curve peak of insulation aging defects (peak 3) increases greatly with aging, while the peak reflecting the interface polarization between the crystalline and amorphous regions of the insulator (peak 2) increases slightly. Furthermore, although the initial value of the relaxation current decreased after one year of aging in water, the significant increase in $I(t) \cdot t$ indicated that aging in water leads to an increase in trap density.

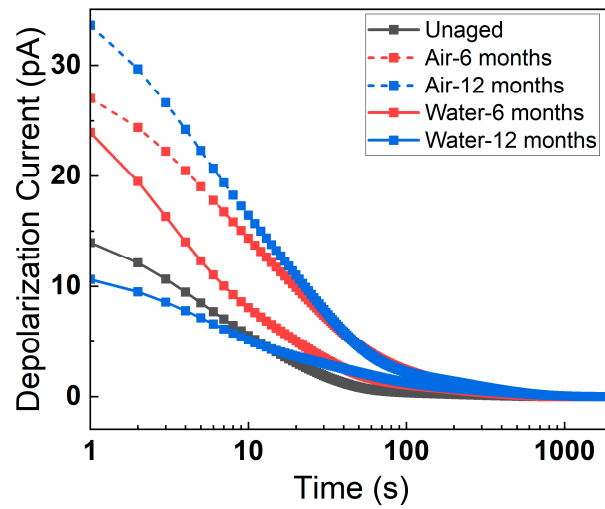


Figure 12. IRC curve of the tested cables with different conditions.

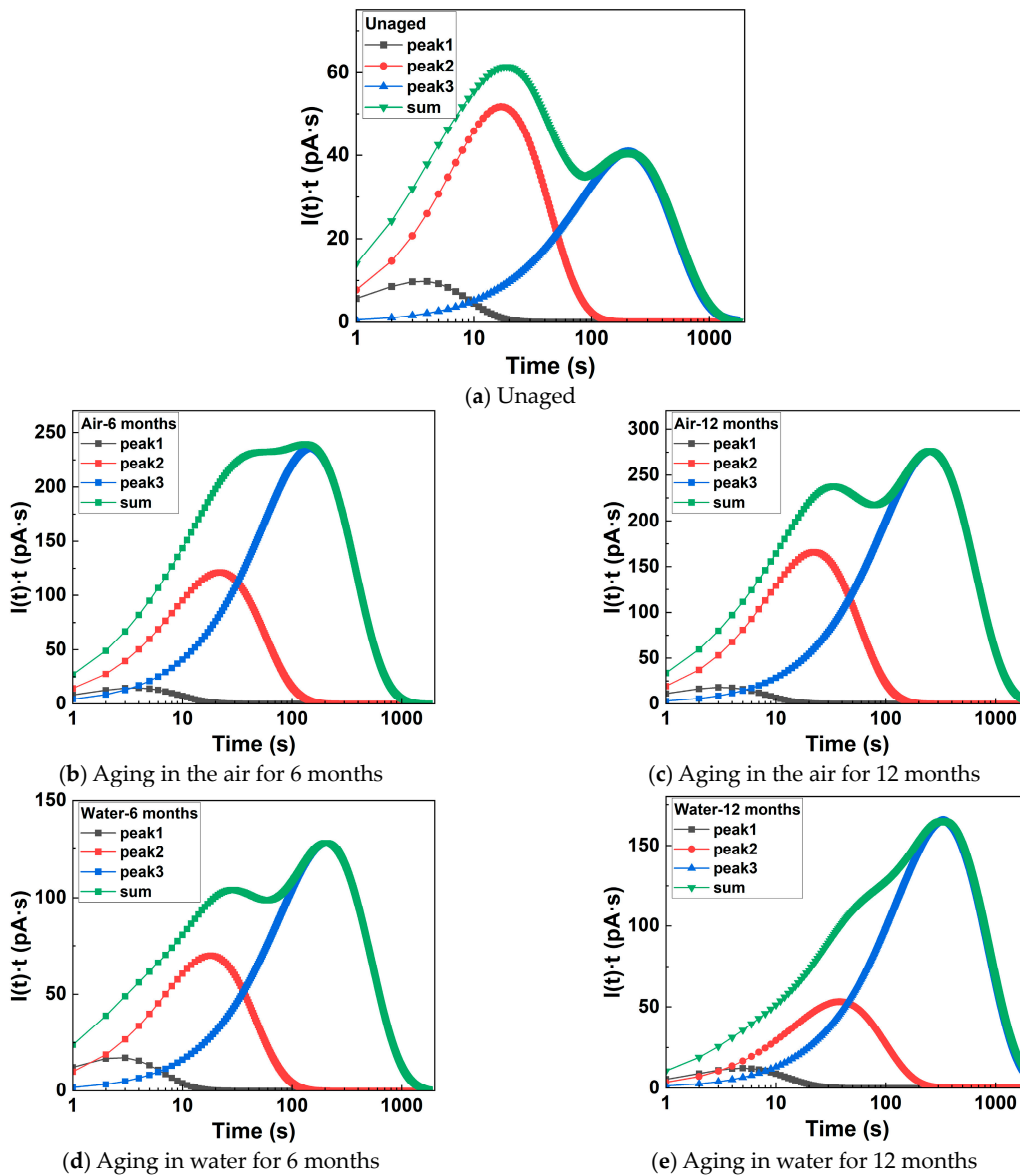


Figure 13. IRC fitting results of tested cables with various aging conditions.

The difference between aging in air and water mainly lies in the shape of $I(t) \cdot t$. When the aging time is 12 months, the sample aged in the air has two obvious peaks, while the sample aged in water gradually evolves into a single peak, indicating that the proportion of peak 3 related to defects and deep depressions is greater in the water-aged cable than in the air-aged cable. In terms of the magnitude of $I(t) \cdot t$, the degree of aging in water is smaller than that in air. It is most likely caused by differences in ambient temperatures during cable aging. The heat dissipation effect of water is significantly stronger than that of air, so the insulation temperature in the air is much higher. Therefore, the effect of thermal aging in air on cable insulation is stronger than that in water, which is consistent with the actual situation. It is worth noting that this phenomenon can also be seen from the interface polarization terms of the crystalline and amorphous regions related to the cable insulation morphology. Judging from the peak value of the interface polarization term between the crystalline region and the amorphous region and its change with aging, the aging of the cable in air is greater than that in water.

To compare the aging degrees of the cables of different aging conditions, the aging factor A , time constants τ , and polarization factor $Q(\tau)$ are calculated, as shown in Table 2.

Table 2. Comparison of fitting parameters of different aging conditions.

Parameters	Unaged	Water		Air	
		6 Months	12 Months	6 Months	12 Months
I_0	−2.88	−2.61	−2.68	−2.93	−2.69
τ_1	3.558	2.62	4.92	3.7	3.2
α_1	7.508	17.99	6.82	10.87	15.41
τ_2	17.1	18.03	37.96	21.88	22.26
α_2	8.22	10.54	3.81	15.07	20.24
τ_3	204.68	204.68	332.59	146.61	253.52
α_3	0.54	1.7	1.35	4.37	2.96
$Q(\tau_2)$	124.42	196.46	173.4	337.51	397.29
$Q(\tau_3)$	237.3	456.36	461.4	774.58	974.96
A	1.91	2.32	2.66	2.29	2.45

The time constant does not change much with the increase in aging time. This means that the trap depth does not deepen during the aging process and the mechanism does not fundamentally change. Regardless of the aging environment, the aging coefficient increases with aging. Judging from the growth rate of aging factors, the contribution of aging factors in water is higher than that of aging factors in air.

5. Conclusions

This paper proposes an improved IRC measurement method based on an isolated circuit, which discharges the interference current from the high-voltage insulated wire back to the earth and reduces the measurement error of depolarization current. At the same time, a three-phase IRC simultaneous test system is designed, and the control software is developed. Furthermore, by verifying the accuracy of the test system, the independence of the single-phase circuit and the consistency of the three-phase circuit is achieved. The influence factors of the IRC test, depolarization time, and test temperature are explored to determine the suitable parameter of further tests. The system is then used to evaluate the aging state of 10 kV cables with various aging conditions in the air and water. The following conclusions can be drawn:

(1) The isolated circuit can effectively avoid the interferences from depolarization of the test system itself such as high-voltage insulated wire. Further, the independence and accuracy of the three-phase IRC detection system were verified, which showed the feasibility of this system.

(2) Depolarization time significantly affects the time constant τ_3 of IRC. When the depolarization time is in the range of 1200~1800 s, the accuracy of IRC results can be effectively improved and the calculated aging factors A are consistent. With the rise in temperature, the depolarization current tends to increase first and then decrease, which is related to the detrapping of charges.

(3) Aging under different laying environments will lead to an increase in trap density in the insulation, aggravating the aging of the cables. Thermal aging in the air has a stronger impact on cable insulation than in water for the same heating current.

Author Contributions: Writing—original draft: H.G. and X.Z.; investigation: B.S., Z.L. and X.W.; Methodology: Y.Z. (Yongkang Zhang) and Y.Z. (Yunjie Zhou); Supervision: Y.W.; writing—review and editing, Y.W. All authors have read and agreed to the published version of the manuscript.

Funding: This research was funded by the Project of State Grid Shanghai Municipal Electric Power Company: SGTYHT/21-JS-223.

Data Availability Statement: The data are available and explained in this article, and readers can access the data supporting the conclusions of this study.

Conflicts of Interest: The authors declare that this study received funding from State Grid Shanghai Municipal Electric Power Company. The funder was not involved in the study design, collection, analysis, interpretation of data, the writing of this article or the decision to submit it for publication.

References

1. Zhou, Y.; Peng, S.; Hu, J.; He, J. Polymeric insulation materials for HVDC cables: Development, challenges, and future perspective. *IEEE Trans. Dielectr. Electr. Insul.* **2017**, *24*, 1308–1318. [[CrossRef](#)]
2. Wang, Y.; Wu, J.; Yi, S.; Yin, Y. Research of simultaneous measurement of space charge and conduction current in cross-linked polyethylene. In Proceedings of the 2016 International Conference on Condition Monitoring and Diagnosis (CMD), Xi'an, China, 25–28 September 2016.
3. Ghorbani, H.; Jeroense, M.; Olsson, C.; Saltzer, M. HVDC Cable Systems—Highlighting Extruded Technology. *IEEE Trans. Power Deliv.* **2014**, *29*, 414–421. [[CrossRef](#)]
4. Wang, Y.; Wu, J.; Yin, Y. Space charge behavior in low density polyethylene at low temperatures. *IEEE Trans. Dielectr. Electr. Insul.* **2017**, *24*, 3860–3868. [[CrossRef](#)]
5. Iddrissu, I.; Lv, Z.; Rowland, M. The dynamic character of partial discharge in epoxy resin at different stages of treeing. In Proceedings of the 2016 IEEE International Conference on Dielectrics (ICD), Montpellier, France, 3–7 July 2016.
6. Shekhar, A.; Feng, X.; Gattozzi, A.; Hebner, R.; Wardell, D.; Strank, S.; Rodrigo-Mor, A.; Ramírez-Elizondo, L.; Bauer, P. Impact of DC voltage enhancement on partial discharges in medium voltage cables—An empirical study with defects at semicon-dielectric interface. *Energies* **2017**, *10*, 1968. [[CrossRef](#)]
7. Mazzanti, G.; Castellon, J.; Chen, G.; Fothergill, J.C.; Fu, M.; Hozumi, N.; Lee, J.H.; Li, J.; Marzinotto, M.; Mauseth, F.; et al. The insulation of HVDC extruded cable system joints. Part 1: Review of materials, design and testing procedures. *IEEE Trans. Dielectr. Electr. Insul.* **2019**, *26*, 964–972. [[CrossRef](#)]
8. Kwaaitaal, T.; Eijnden, W. Dielectric loss measurement as a tool to determine electrical aging of extruded polymeric insulated power cables. *IEEE Trans. Electr. Insul.* **2007**, *EI-22*, 101–105. [[CrossRef](#)]
9. Kim, C.; Jin, Z.; Jiang, P.; Zhu, Z.; Wang, G. Investigation of dielectric behavior of thermally aged XLPE cable in the high-frequency range. *Polym. Test.* **2006**, *25*, 553–561. [[CrossRef](#)]
10. Fothergill, J.; Dodd, S.; Dissado, L.; Liu, T.; Nilsson, U.H. The measurement of very low conductivity and dielectric loss in XLPE cables: A possible method to detect degradation due to thermal aging. *IEEE Trans. Dielectr. Electr. Insul.* **2011**, *18*, 1544–1553. [[CrossRef](#)]
11. Li, Z.; Du, B. Polymeric insulation for high-voltage dc extruded cables: Challenges and development directions. *IEEE Electr. Insul. Mag.* **2018**, *34*, 30–43. [[CrossRef](#)]
12. Lee, J.; Jeong, W.; Dinh, M.; Yu, I.-K.; Park, M. Comparative Analysis of XLPE and Thermoplastic Insulation-Based HVDC Power Cables. *Energies* **2023**, *16*, 167. [[CrossRef](#)]
13. Yiwana, A.; Reddy, C. On the Anomalous Charging and Discharging Currents in LDPE under High Electric Fields. *IEEE Trans. Dielectr. Electr. Insul.* **2018**, *25*, 127–136.

14. Beigert, M.; Kranz, H. Destruction free ageing diagnosis of power cable insulation using the isothermal relaxation current analysis. In Proceedings of the IEEE Conference on International Symposium on Electrical Insulation (ISEI), Pittsburgh, PA, USA, 5–8 June 1994.
15. Simmons, J.; Tam, M. Theory of isothermal currents and the direct determination of trap parameters in semiconductors and insulators containing arbitrary trap distributions. *Phys. Rev. B* **1973**, *7*, 3706–3713. [[CrossRef](#)]
16. Birkner, P. Field experience with a condition-based maintenance program of 20 kV XLPE distribution system using IRC-analysis. *IEEE Trans. Power Deliv.* **2004**, *19*, 3–8. [[CrossRef](#)]
17. Zhu, X.; Yin, Y.; Wu, J.; Wang, X. Study on Aging Characteristics of XLPE Cable Insulation Based on Quantum Chemical Calculation. *IEEE Trans. Dielectr. Electr. Insul.* **2020**, *27*, 1942–1950. [[CrossRef](#)]
18. Wang, Y.; Wu, J.; Yin, Y. A space-charge and relaxation-current based method for estimating electron and hole trap energy distribution. *IEEE Trans. Dielectr. Electr. Insul.* **2017**, *24*, 3839–3848. [[CrossRef](#)]
19. Wu, J.; Yin, Y.; Li, X.; Wang, Y.; Xiao, D. The condition assessment -system of XLPE cables using the isothermal relaxation current technique. In Proceedings of the 2009 IEEE International Conference on the Properties and Applications of Dielectric Materials (ICPADM), Harbin, China, 19–23 July 2009.

Disclaimer/Publisher’s Note: The statements, opinions and data contained in all publications are solely those of the individual author(s) and contributor(s) and not of MDPI and/or the editor(s). MDPI and/or the editor(s) disclaim responsibility for any injury to people or property resulting from any ideas, methods, instructions or products referred to in the content.